Polarized pressure dependence of the anisotropic dielectric functions of highly oriented poly(p-phenylene vinylene)

V. Morandi,[1,a)] M. Galli,[1] F. Marabelli,[1] and D. Comoretto[2]
[1]*Dipartimento di Fisica "A.Volta," Università degli Studi di Pavia, Via Bassi 6, Pavia 27100, Italy*
[2]*Dipartimento di Chimica e Chimica Industriale, Università di Genova, via Dodecaneso 31, Genova 16146, Italy*

(Received 2 July 2009; accepted 26 January 2010; published online 7 April 2010)

In this work, we combined an experimental technique and a detailed data analysis to investigate the influence of an applied pressure on the anisotropic dielectric functions of highly oriented poly(p-phenylene vinylene) (PPV). The dielectric constants were derived from polarized reflectance spectra recorded through a diamond anvil cell up to 50 kbar. The presence of the diamond anvils strongly affects measured spectra requiring the development in an optical model able to take all spurious effects into account. A parametric procedure was then applied to derive the complex dielectric constants for both polarizations as a function of pressure. A detailed analysis of their pressure dependence allows addressing the role of intermolecular interactions and electron-phonon coupling in highly oriented PPV. © *2010 American Institute of Physics*. [doi:10.1063/1.3330171]

I. INTRODUCTION

Highly oriented poly(p-phenylene vinylene) (PPV) is an ideal playground to investigate the fundamental photophysical properties of conjugated systems. PPV is indeed a reference material in the field of organic optoelectronics[1] and has been widely studied since the early discovery of electroluminescence in semiconducting polymers.[2] Furthermore, the availability of highly oriented samples with good optical quality offers the unique opportunity to probe the anisotropic optical and electronic properties with minor effects related to disorder. As a matter of fact, the stretching procedure deeply affects the polymer microstructure.[3] Due to tensile drawing, an axial symmetry is induced (originating from the alignment of the macromolecules) and ordered crystalline regions are created (~70%).[3]

A detailed optical characterization of highly oriented PPV carried out with a variety of spectroscopic techniques[4–9] provided an unambiguous assignment of the main spectral features. In particular, on one hand, polarized optical spectroscopy joined to theoretical calculations allowed assigning the electronic transitions for isolated chains. On the other hand, photoluminescence (PL) anisotropy showed the existence of two emitting states,[6] that were suggested to be correlated with the crystalline and amorphous regions coexisting in this sample.[3] In the amorphous regions, the electronic transitions might originate mainly from isolated macromolecules, while in the crystallites, intermolecular interaction would influence the electronic structure of PPV, changing the polarization properties of the corresponding emission. These results are in agreement with emission studies on PPV-silica nanocomposites[10] which revealed the presence of two emitting states: The main one, gaining intensity upon increasing the silica load, was assigned to the isolated molecular state, whereas the lower lying emission was attributed to an aggregate (interchain) exciton state formed by dipole-dipole coupling of two or more molecular exciton states on different chain segments.

In the analysis previously reported on highly oriented PPV, the determination of the anisotropic optical constants proved to be crucial to better understand of the origin of emission peaks. Indeed, PL spectra are strongly affected by self-absorption, anisotropic reflectance at the sample surface, refraction, and light extraction problems.[6] These issues can only be accounted for by a proper optical model requiring the knowledge of the complex refractive index. The apparent discrepancy between absorption (probing purely intramolecular effects) and emission (intramolecular and intermolecular effects) is related to the higher sensitivity to interchain interactions of the photophysical processes and PL with respect to optical absorption, as already observed in different conjugated polymers.[11,12]

Based on these results, we directly investigated the role of interchain interactions in highly oriented PPV by means of optical spectroscopy under pressure.[13] We showed that deep changes in the oscillator strength occur for both polarization components and we observed a modification of the role of electron-phonon (el-ph) coupling relative to intermolecular effects. This achievement was possible through the study of the pressure dependence of the anisotropic complex dielectric functions ($\tilde{\epsilon}=\epsilon_1+i\epsilon_2$) of oriented PPV, derived from reflectance spectra measured through a diamond anvil cell (DAC).

As a first step to determine the complex dielectric constants of stretch oriented PPV, an optical model of our system is needed. Indeed, besides the sample response, several other contributions affect measured reflectance spectra. A reflection contribution of the front diamond of the DAC as well as the dielectric contrast between diamond and sample (instead of the usual air/sample interface) must be taken into account. In addition, the optical transfer function specific of our DAC has to be considered. Despite the small angular

a)Electronic mail: valentina.morandi@gmail.com.

divergence (1°) of the incident beam, diamond birefringence causes a mixing of the polarization components that can only be accounted for with specific calibration measurements on the empty cell.

Once reliable renormalized reflectance spectra have been obtained for both polarizations, we faced with the problem of extracting the complex dielectric function components. Since, due to the limited spectral range that could be detected, a direct Kramers–Kronig (KK) analysis of the spectra did not provide reliable results, it was then necessary to develop a parametric method to derive the polarized components of $\tilde{\epsilon}$.

Aim of this work is to describe in detail the optical model used for data analysis as well as the parametric procedure through which the anisotropic dielectric constants were obtained.

II. EXPERIMENTAL

A thick, stretch-oriented film of PPV was studied in this work. A description of its structure as well as of the synthetic and stretching procedures used to obtain it can be found in Ref. 3 and references quoted therein. The experimental details of the set up used to perform polarized reflectance (R) measurements and of the DAC have been already described elsewhere.[13] Incident light was polarized either parallel or perpendicular to the polymer chain axis, aligned to the stretching direction. It is important to point out that the optical system provided a probing spot of 50 μm with an angular divergence of the incident light cone of less than 1°. Such a small beam size allowed improving the control on polarization through the diamond. A separate control experiment was performed to monitor the hydrostatic character of applied pressure using CsI as pressure transmitting medium and ruby emission as pressure gauge. Within the pressure range explored, the R_1 linewidth of ruby shows an increase in only 5%, indicating the good hydrostatic conditions of our measurements.

III. RESULTS AND DISCUSSION

A. Reflectance spectra

Figure 1 shows measured reflectance spectra for different applied pressures, with light polarization parallel and perpendicular to the polymer chains. Many features of the reflectance spectra are reminiscent of the previous extended optical characterization of highly oriented PPV (Refs. 4–8) and point out that this sample possesses an exceedingly extended conjugation length and a high degree of structural order. In Fig. 1(a) these features are the low energy of the $\pi-\pi^*$ transition (at 2.46 eV, 504 nm), the clear resolution of the vibronic replicas (at 2.70–2.90–3.09 eV, 460–427–401 nm) and the weakness of the structure associated with the so-called peak II (indicated by an arrow in Fig. 1(a) at 3.77 eV, 329 nm), ascribed to conjugation chain ends.[5,14,15] Moreover, a strong anisotropy of R spectra is observed.

These features exhibit a smooth spectral evolution upon increasing pressure, thus allowing us to discuss the pressure dependence of the main spectral features from raw data. For instance, as an effect of pressure, a rigid redshift in all optical transitions is detected in both the parallel and perpendicular component (Fig. 1). This effect, already observed in different conjugated polymers under pressure,[16–18] can in principle result from an interplay of two different phenomena: An increase in the average conjugation length of the polymer, due to a planarization of its backbone, and an increase in wave function delocalization on neighboring chains favored by the reduction in interchain distances. In disordered materials, intrachain effects usually prevail and mask any contribution due to an enhancement of interchain interactions. Pioneering work on PPV oligomers[19,20] showed that their optical properties are strongly affected by conjugation length, which in turn is related to chain planarity. The changes observed in the relative intensity of Raman peaks associated with C—C and C═C stretching of the phenyl ring and with C═C stretching of the vinylene group were ascribed to differences in the effective intramolecular conjugation length. However, this is not the case for highly oriented PPV. As a matter of fact, Raman spectroscopy on the same sample showed that pressure causes no planarization of the polymer chains, thus inducing a negligible increase in its conjugation length.[13] Furthermore, different pressure-induced redshifts in the $\pi-\pi^*$ transition and of peak II [−3.7 and −2.7 meV/kbar, respectively, Fig. 1(a)] were detected. It is important to notice that in PPV peak II borrows intensity from the $\pi-\pi^*$ transition as a consequence of purely intramolecular effects, while in its derivatives a contribution from symmetry breaking due to electroactive substituents also occurs.[5,14,15,21] On the other hand, the $\pi-\pi^*$ transition is very sensitive to both conjugation length extension (intramolecular effect) and interchain interactions. Close inspection of the data suggests that such a transition splits into two components upon increasing pressure (see inset of Fig. 1, showing the second derivative of parallel reflectance

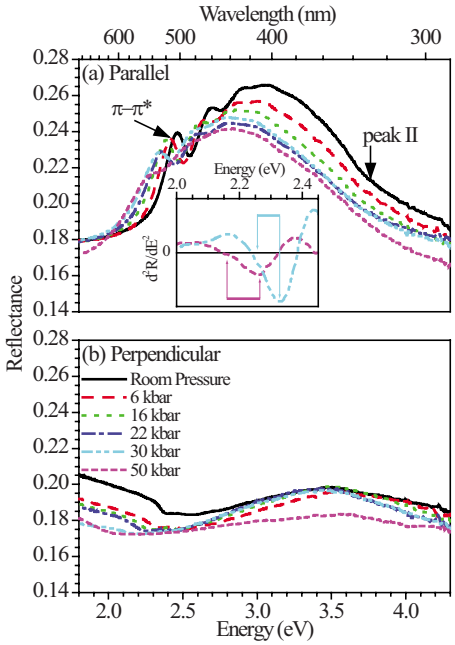

FIG. 1. (Color online) Measured reflectance spectra of highly oriented PPV for the (a) parallel and (b) perpendicular polarization at different applied pressures. Inset: second derivative spectrum of R parallel for the two highest applied pressures.

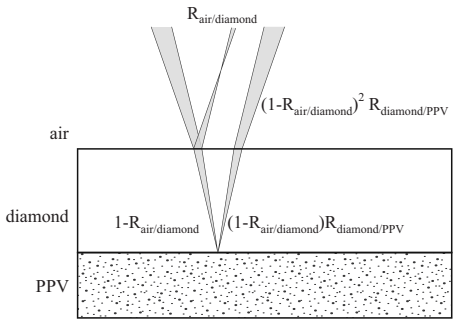

FIG. 2. Schematic of the model used to analyze reflectance spectra.

spectra recorded at the two highest pressures). These observations lead us to infer that, due to its stronger pressure dependence with respect to peak II, the $\pi-\pi^*$ transition is affected by more complicated mechanisms.[13] These phenomena could be investigated in detail only by analyzing the complex dielectric functions obtained after removing from measured spectra any spurious effect due to the DAC optical response. As a matter of fact, besides the features discussed above, the spectra in Fig. 1 exhibit also some remarkable differences with respect to the literature data for the same sample recorded without the cell.[4–6,8] Such differences arise from contributions to reflectance from both the diamond surface and PPV/diamond interface. Besides altering the intensity of R spectra, the refractive index of diamond also affects their shape, which is further modified by the polarization mixing introduced by diamond birefringence. This effect is particularly apparent in the perpendicular component [Fig. 1(b)], due to its weak intensity, and is revealed by the presence of an anomalous structure at ~3.5 eV. In order to separate these spurious contributions from the sample response, it was necessary to develop an optical model providing the purely parallel and perpendicular components of R spectra (Sec. III B).

B. Model for reflectance analysis

The main contributions affecting measured spectra are: reflection from the front surface of the DAC; the dielectric contrast between diamond and sample instead of the usual air/sample interface, and the optical transfer function of our DAC, in particular, diamond birefringence. To account for these effects, caused by the presence of the diamond, the system was modeled as composed by three media (PPV, diamond, and air), with different refractive indexes, as depicted in Fig. 2, where contributions to the optical signal from the various interfaces are sketched. The experimental reflectivity R_{exp} can be expressed as:

$$R_{exp} = R_{air/diamond} + (1 - R_{air/diamond})^2 R_{diamond/PPV}$$
$$= R_{air/diamond} + T_{air/diamond/air} R_{diamond/PPV}. \quad (1)$$

The first term $R_{air/diamond}=[(1-n_{diamond})/(1+n_{diamond})]^2$, accounts for the air/diamond interface reflectivity, where the diamond refractive index dispersion[22] was also taken into account. This is the only additive term. The second term in Eq. (1) expresses the reflectivity contribution of the diamond/PPV interface weighted by diamond transmittance

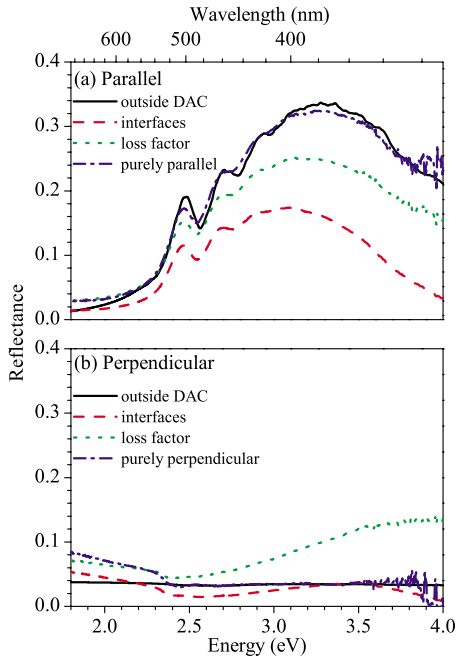

FIG. 3. (Color online) Room pressure reflectance spectra for the (a) parallel and (b) perpendicular polarization after each step of the mathematical modeling used for data analysis. Black solid spectra labeled "outside DAC" refer to reflectance of a PPV/diamond interface as derived from the optical functions of PPV reported in Refs. 4–7.

as represented in Fig. 2. Higher order terms, arising from multiple reflections between the interfaces can be estimated to contribute less then 1% and are neglected in this model. Reflectance $R_{diamond/PPV}$ of PPV derived from experimental data through Eq. (1) is plotted in Fig. 3 for both polarization components and compared to the ideal reflectance of a PPV/diamond interface calculated using literature data for both oriented PPV (Refs. 4–7) and diamond refractive index.[22] Even when the air/diamond interface is considered via Eq. (1), room pressure reflectance measured through the DAC presents a lower intensity with respect to the calculated one (Fig. 3). In particular, the intensity of the parallel component is lower in the whole spectral range, with a greater decrease in the high energy region. The perpendicular component, rather than being flat with an absolute value ~3%, has a swinging behavior, indicating its higher sensitivity to spurious contributions with respect to the parallel one. These spurious effects are related to the optical response of the DAC, whose reflectance cannot be simply reproduced using literature data for the diamond refractive index.[22] Figure 4(a) shows the DAC polarized reflectance measured focusing the probe beam onto its back surface (culet), as compared with reflectance calculated[22] assuming contributions from the air/diamond interface only (lower, dashed line) and from both air/diamond+diamond/air interfaces (upper, solid line). A remarkable difference in both absolute value and dispersion is observed. In particular, it can be notice that the experimental spectra lie in between the calculated ones. This discrepancy is due to the extended depth of field of our optical set-up, caused by the small angular divergence of incident beam, that allows only a partial detection of the contribution to reflectance of the front diamond surface (see Fig. 2). A

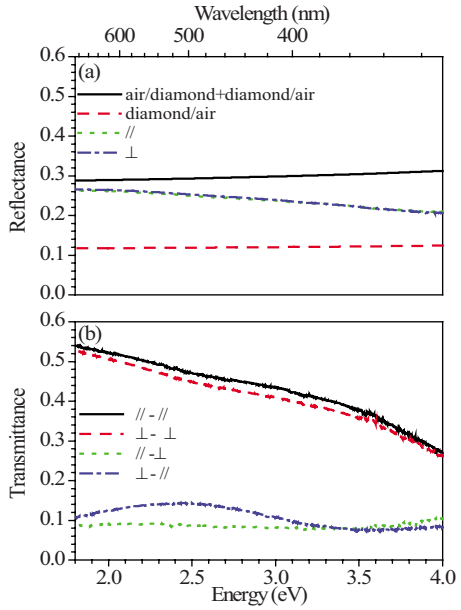

FIG. 4. (Color online) (a) Polarized reflectance of the front diamond of the DAC measured focusing the probe beam onto its back surface (culet). Reflectance spectra calculated (Ref. 22) assuming contributions from the air/diamond interface only (lower, dashed line) and from both air/diamond+diamond/air interfaces (upper, solid line) are shown for comparison. (b) Transmittance through the front diamond of the DAC in a double polarizer experiment. The symbols refer to polarizer and analyzer polarization, respectively.

direct characterization of the DAC optical response is thus the more convenient and reliable way to account for this effect.

In order to estimate the intensity loss, reflectance, and transmittance of the empty cell have been measured. A loss factor α has been experimentally evaluated from the total reflectivity of the empty DAC using the relation:

$$R_{\mathrm{exp}}^{\mathrm{emptyDAC}} = \alpha R_{\mathrm{air/diamond}} + \alpha^2(1 - R_{\mathrm{air/diamond}})^2 R_{\mathrm{diamond/air}} = \alpha R_{\mathrm{air/diamond}} + \alpha^2 T_{\mathrm{air/diamond/air}} R_{\mathrm{diamond/air}}, \quad (2)$$

where $T_{\mathrm{air/diamond/air}}$ is the transmittance through the double air/diamond interface and $R_{\mathrm{air/diamond}}$ is the ideal reflectance of the air/diamond interface used in Eq. (1). Once α is known over the entire spectral range, PPV reflectivity for both polarizations can be obtained from the following:

$$R_{\mathrm{diamond/PPV}} = \frac{R_{\mathrm{exp}} - \alpha R_{\mathrm{air/diamond}}}{\alpha^2 T_{\mathrm{air/diamond/air}}} = R_{\mathrm{PPV}}, \quad (3)$$

where R_{exp} is the experimental reflectivity of PPV measured through the DAC, and α is obtained via Eq. (2). For sake of brevity, hereafter we will refer to $R_{\mathrm{diamond/PPV}}$ in Eq. (3) as R_{PPV}.

The phenomenological loss factor α modifies both the intensity and spectral shape of the two polarization components of R spectra, as shown in Fig. 3. However, the agreement between experimental and ideal reflectance spectra still remains unsatisfactory. In particular, the parallel component is lower than expected on the whole spectral range; the opposite occurs for the weak perpendicular component. This effect is related to the strain-induced diamond birefringence[23] which causes an inhomogeneous rotation of the plane of polarization and is particularly relevant in the study of anisotropic samples, such as oriented PPV.

In order to clarify this issue, a double polarizer transmittance measurement of the front diamond alone was performed. Transmitted light was found to be nonzero with crossed polarizers, showing a strong spectral dependence [Fig. 4(b)].

Assuming the same polarization mixing occurs for all applied pressures,[24] the amount of mixing can be determined by the coefficients:

$$a = \frac{T^{\parallel-\parallel}}{T^{\parallel-\parallel} + T^{\parallel-\perp}}, \quad (4a)$$

$$b = \frac{T^{\perp-\perp}}{T^{\perp-\perp} + T^{\perp-\parallel}}, \quad (4b)$$

being T the transmittance of the DAC front diamond [Fig. 4(b)], where the symbols refer to polarizer and analyzer, respectively

The recorded polarized components [R_{PPV} in Eq. (3)], affected by polarization mixing, can be expressed as:

$$R_{\mathrm{PPV}}^{\parallel}(\mathrm{mix}) = aR_{\mathrm{PPV}}^{\parallel} + (1-a)R_{\mathrm{PPV}}^{\perp}, \quad (5a)$$

$$R_{\mathrm{PPV}}^{\perp}(\mathrm{mix}) = bR_{\mathrm{PPV}}^{\perp} + (1-b)R_{\mathrm{PPV}}^{\parallel}, \quad (5b)$$

where $R_{\mathrm{PPV}}^{\parallel}$ and $R_{\mathrm{PPV}}^{\perp}$ are the purely parallel and perpendicular reflectance spectra of PPV, which can be obtained inverting Eqs. (5a) and (5b)

$$R_{\mathrm{PPV}}^{\parallel} = \frac{1}{1-a-b}[(1-a)R_{\mathrm{PPV}}^{\perp}(\mathrm{mix}) - bR_{\mathrm{PPV}}^{\parallel}(\mathrm{mix})]. \quad (6a)$$

$$R_{\mathrm{PPV}}^{\perp} = \frac{1}{1-a-b}[(1-a)R_{\mathrm{PPV}}^{\parallel}(\mathrm{mix}) - bR_{\mathrm{PPV}}^{\perp}(\mathrm{mix})]. \quad (6b)$$

It is important to notice that, as a result of the modeling so far described, an increase in the noise level of the spectra is apparent for high energies (Fig. 3), limiting, in the most conservative scenario, the spectral reliability of our data up to 3.5 eV. Moreover, due to its low intensity the perpendicular component is more sensitive to uncertainties, thus any feature in these spectra requires a more careful interpretation. Despite the overall good agreement achieved after corrections between room pressure R spectra measured through and without the DAC (Fig. 3), minor discrepancies still remain. These differences are probably ascribed to light scattering of the sample itself, as inferred from previous spectroscopic measurements[6] and cannot be here accounted for without severe arbitrary assumptions. We remark that the correction procedure applied to measured reflectance spectra relies on a detailed experimental calibration of the cell and no adjustable parameters have been introduced.

C. Dielectric constants

The limited spectral range of our data prevents a direct KK determination of reliable complex dielectric functions from PPV reflectance spectra. For this reason, a KK compatible parametric procedure was developed to derive the anisotropic complex dielectric constants ($\tilde{\epsilon} = \epsilon_1 + i\epsilon_2$). The dielec-

tric functions of oriented PPV, obtained with a KK analysis in a previous study,[5–7] were used as a starting point to determine the parametric form of $\tilde{\epsilon}$, as described in the following.

As a first step, the imaginary part of the dielectric constant (ϵ_2) was expressed as a sum of Gaussians[25]

$$\epsilon_2 = \sum_i^{11} a_i e^{[-(p_i - x/\gamma_i)^2]}, \tag{7}$$

where p_i is the energy position of the ith peak, a_i is its height, and γ_i is related to its half width at half maximum $\mathrm{HWHM}_i = \gamma_i\sqrt{\ln 2}$. The KK transform of a Gaussian [or of a sum of Gaussians as in Eq. (7)] is an integral function with no analytic form. We thus fitted (within 1% in the spectral range of interest) this function with the following analytic expression, depending on the same fitting parameters as the Gaussian curve

$$z_i = \frac{1.1943(q_i^2 - x^2)a_i q_i \gamma_i}{(q_i^2 - x^2)^2 + (1.876\gamma_i)^2 x^2} + 4.3099 a_i e^{[-(q_i - 0.05\gamma_i - x/1.3\gamma_i)^2]} - 4.3099 a_i e^{[-(q_i + 0.05\gamma_i - x/1.3\gamma_i)^2]}, \tag{8}$$

being

$$q_i = p_i\left[1 + 0.225\left(\frac{\gamma_i}{p_i}\right)^2\right]. \tag{9}$$

Hence, ϵ_1 could be built as a sum of analytic functions:

$$\epsilon_1 = \epsilon_{\mathrm{inf}} + \sum_i^{11} z_i, \tag{10}$$

where ϵ_{inf} is the residual value of ϵ_1 due to electronic transitions of energy higher than the investigated spectral range.

Equations (7) and (10) provide a KK compatible parametric form of $\tilde{\epsilon}$, that allowed reproducing the dielectric constant spectrum obtained outside the DAC as a function of p_i, a_i, and γ_i. PPV reflectance measured through the DAC can be obtained through the following expression:

$$R = \frac{\sqrt{\epsilon_1^2 + \epsilon_2^2} - n_{\mathrm{diamond}}\sqrt{2(\epsilon_1 + \sqrt{\epsilon_1^2 + \epsilon_2^2})} + n_{\mathrm{diamond}}^2}{\sqrt{\epsilon_1^2 + \epsilon_2^2} + n_{\mathrm{diamond}}\sqrt{2(\epsilon_1 + \sqrt{\epsilon_1^2 + \epsilon_2^2})} + n_{\mathrm{diamond}}^2} \tag{11}$$

using the variables p_i, a_i, and γ_i as free parameters in a best fitting routine and n_{diamond} from literature.[22] Due to the good agreement achieved through the previous correction procedure, the ambient pressure spectrum was obtained with a minimal parameter adjustment. As a second step we derived the anisotropic components of $\tilde{\epsilon}$ from R spectra under pressure. Each reflectivity spectrum was reproduced determining the optimal set of parameters p_i, a_i, and γ_i. Then, ϵ_1 and ϵ_2 could be obtained through Eqs. (7) and (10). The fitting was progressively applied to obtain $\tilde{\epsilon}$ at higher pressures and a smooth evolution of the fit parameters was ensured initializing the fit with the values determined for the preceding pressure. The number of Gaussians (hence the number of fitting parameters) was chosen to be the minimum allowing to mimic accurately R for each applied pressure.

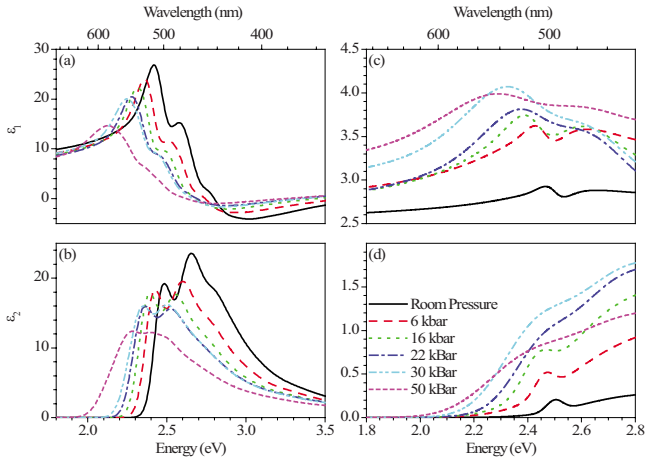

FIG. 5. (Color online) Parallel (left panels) and perpendicular (right panels) component of the real (upper panels) and imaginary (lower panels) part of the dielectric constant.

Figure 5 shows the real and imaginary part of the dielectric constant (ϵ_1 and ϵ_2 in the upper and lower panels, respectively) for the parallel and perpendicular polarization (left and right panels, respectively).

The parallel component (Fig. 5) shows the lowest energy peak in ϵ_1 at 2.42 eV (512 nm) while the following peaks are at 2.58 eV (481 nm) and 2.77 eV (448 nm). The $\pi-\pi^*$ transition is detected in ϵ_2 at 2.48 eV (500 nm) at room pressure, followed by its vibronic replica at 2.65 eV (468 nm) and 2.81 eV (441 nm).

Due to the low absolute value of R spectra with polarization perpendicular to the chain axis [Fig. 1(b)], the complex dielectric constants with this polarization (Fig. 5) have a much weaker intensity (notice vertical scale) than the parallel counterparts, and are thus intrinsically affected by a grater uncertainty. In particular, in both ϵ_1 and ϵ_2 shown in Fig. 5 two structures can be detected around 2.5 eV that have been assigned to a projection, caused by chain misalignment, of parallel component of this transition into the perpendicular direction.

In general, all transitions undergo a bathochromic shift with increasing pressure. The 0–0, 0–1, and 0–2 vibronic transitions in $\tilde{\epsilon}$ parallel show a pressure dependence comparable to previous findings from R spectra (Fig. 1) reported in Ref. 13. The shift rate of the feature at ~2.5 eV in $\tilde{\epsilon}$ perpendicular is similar to that of the $\pi-\pi^*$ transition observed in the parallel component, thus confirming its origin being due to chain misalignment.

Besides a redshift, an additional effect of pressure, clearly detectable in Fig. 5, is a broadening of all the vibronic transitions. This effect, already observed in R spectra (Fig. 1), was attributed to the interplay between enhanced interchain interactions and el-ph coupling. A qualitative evaluation of the relative strength of intermolecular interaction and el-ph coupling was provided in Ref. 13.

The overall influence of pressure on $\tilde{\epsilon}$ is remarkably different for the parallel and perpendicular polarization. This is particularly apparent when comparing the imaginary parts of both polarizations (lower panel of Fig. 5). Upon applying pressure, the overall intensity of the parallel component of ϵ_2

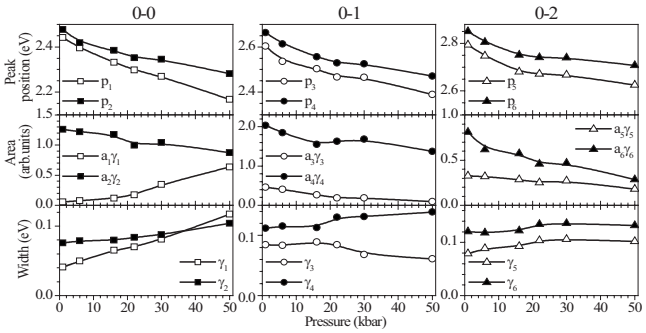

FIG. 6. Pressure dependence of the fitting parameters corresponding to peak positions p_i, areas $a_i\gamma_i$ (in units of $\sqrt{\pi}$), and width γ_i of the Gaussians that form the 0–0, 0–1, and 0–2 transitions. White (black) symbols refer to the lowest (highest) energy component of each doublet.

(Fig. 5) decreases. On the other hand, ϵ_2 with perpendicular polarization (Fig. 5) increases in intensity with pressure, showing a strong enhancement for energies higher than 2.4 eV. This behavior suggests that, as a result of applied pressure, transitions polarized along the chain axis are spread over a wide spectral range (redshift) while those with perpendicular polarization gain intensity, particularly in the high energy region. This effect is clearly evident when the oscillator strength is analyzed and can be related to the enhancement of interchain interactions caused by pressure.[13]

The oscillator strength calculated for highly oriented PPV and reported in Ref. 13 clearly shows in the perpendicular component an intensity increases with pressure above 2.4 eV. This feature might be tentatively assigned to charge transfer states predicted in Ref. 26 for crystalline PPV, where theoretical *ab initio* calculations including electron correlation show that a charge transfer state barely optically active on the perpendicular polarization occurs for energies above the $\pi-\pi^*$ transition.

We can analyze the pressure dependencies of the best-fit parameters for the parallel component only, to provide a deeper, quantitative, and meaningful interpretation of the observed spectral features. As previously discussed, for the sake of caution, we consider the data analysis valid up to 3.5 eV, so we limit the present study to those parameters describing the energy, area, and width of the Gaussians corresponding to the purely electronic transition (0–0) and its vibronic replicas (0–1 and 0–2). Six out of the eleven Gaussians will then be taken into account, that can be separated into three pairs. Each pair accounts for a vibronic peak observed in the experimental spectra.

Figure 6 shows the pressure dependence of the parameters p_i $(i=1\div6)$ corresponding to the energy of the ith peak of the Gaussian in ϵ_2, of γ_i, which refers its width, and of $a_i\gamma_i$ evaluating the area underneath each curve in units of $\sqrt{\pi}$. It's worth noticing that *two* curves, not just one, were necessary to reproduce accurately the $\pi-\pi^*$ transition and each vibronic replica, even at room pressure. At high pressure, this requirement becomes more evident and can be interpreted as a proof of the existence of intermolecular interactions. A better understanding of the role of intermolecular interactions can be achieved studying the behavior of the fitting parameters characterizing each curve.

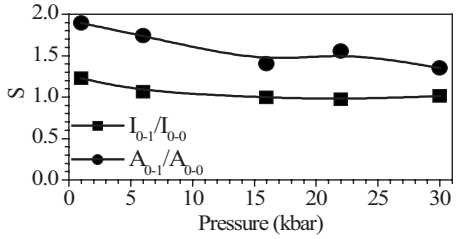

FIG. 7. Pressure dependence of the Huang–Rhys factor estimated through the ratios of the 0–1 and 0–0 peak intensity (I_{0-1}/I_{0-0}) and area (A_{0-1}/A_{0-0}).

Let us consider the parameters corresponding to the purely electronic transition (0–0, left panels in Fig. 6). Upon applying pressure, the doublet necessary to reproduce this structure clearly splits, the separation of the two peaks at 50 kbar being ~110 meV (in agreement with the analysis of R derivatives shown in the inset of Fig. 1). Simultaneously, the area underneath the lowest energy peak p_1 increases with pressure becoming comparable with that of p_2 at 50 kbar. Moreover, a broadening of both Gaussians is also observed at higher pressures, as shown by the parameters γ_1 and γ_2.

From these observations we can conclude that at room pressure the 0–0 transition is mostly due to the high energy peak p_2. On the other hand, when chains are brought closer to each other, the strength of the lower energy peak increases at the expense of the higher energy one. The splitting occurring between the two components might be interpreted as a Davydov splitting caused by the peculiar crystal symmetry of highly oriented PPV, with two inequivalent chains per unit cell. Theoretical *ab initio* calculations of the optical properties of crystalline PPV (Ref. 26) predict an exciton Davydov splitting of 120 meV in agreement with our data where a variation from 35 to 113 meV is observed in the investigated pressure range.

The fit parameters for the 0–1 and 0–2 vibronic replicas also reported in Fig. 6 show a behavior similar to that of the purely electronic transition. The peaks p_i $(i=36)$ composing the 0–1 and 0–2 transitions, separate with increasing pressure. However, the splitting observed is less pronounced than that of p_1 and p_2. In fact, these structures are strongly affected from the surrounding Gaussians reproducing neighboring transitions, thus making any quantitative evaluation of the splitting more difficult. For both doublets, the strong decrease in intensity is counterbalanced by an increase in width, that causes the areas underneath each of these Gaussians to change only slightly with pressure.

The parallel component of ϵ_2 [Fig. 5(b)] provides a deeper insight into the effect of pressure on the el-ph coupling of the system through the Huang–Rhys factor S. A rough evaluation of the Huang–Rhys factors for each applied pressure is given by the ratio of the 0–1 to 0–0 peak intensity (I_{0-1}/I_{0-0}) (Fig. 7). Values of S varying from 1.2 to 1 are found in the investigated pressure range. The results of the fitting procedure allow calculating S in a more accurate way by summing the areas of both structures underneath each peak. The area associated with the purely electronic transition (A_{0-0}) and the vibronic replica (A_{0-1}) used to evaluate S are also plotted in Fig. 7. Upon applying pressure, the Huang–Rhys factors obtained with both methods show a

variation in less than 30%. Even though the absolute values of S could be in principle affected by the optical model used, we notice that its limited dependence on pressure, together with previous findings from Raman spectra,[13] indicate that hydrostatic pressure negligibly affects el-ph interactions in highly oriented PPV. On this basis since pressure was shown to affect negligibly both conjugation length and el-ph coupling in oriented PPV,[13] we deduce that the main variations in optical spectra are due to interchain interactions, which increase in an order of magnitude in the applied pressure range (see Fig. 6 and Ref. 13.) Since the conjugation length of this sample is noticeably extended and since it was recently shown that exciton coupling is reduced upon increasing the conjugation length,[27] we conclude that the values of intermolecular coupling here evaluated can be considered as the lower limit in the field of conjugated polymers.

IV. CONCLUSIONS

The optical properties of oriented PPV were studied by means of polarized reflectance recorded at different applied pressures. A suitable optical model was developed to remove from the spectra spurious effects due to the presence of diamond, altering both the intensity and shape of reflectance spectra. Using a parametric KK compatible procedure, it was possible to obtain the complex dielectric functions for both polarizations at each applied pressure.

The Huang–Rhys factors evaluated from the parallel component of ϵ_2 show minor variations in the investigated pressure range. On the other hand, the intermolecular interactions bandwidth increases by an order of magnitude over the applied pressure range. Therefore, interchain coupling is responsible for the main variations observed in the optical spectra. Furthermore, the analysis of the fit parameters reveals that each vibronic transition is composed by a doublet. The effect of pressure is to further split the two components of each transition, which can be interpreted as Davydov splitting induced by the modulation of interchain distances. Transfer of oscillator strength to the perpendicular component of ϵ_2 is also observed, that could be attributed to charge transfer states, whose existence was recently suggested in Ref. 26.

ACKNOWLEDGMENTS

Financial support was provided by the Ministry of Instruction, University, and Research through the project FIRB 2003 "Synergy," Project No. RBNE03S7XZ. V.M. acknowledges grant from Regione Lombardia (Project No. REGLOM16). The authors are grateful to Professors R. Bini and M. Patrini for helpful discussions.

[1] N. Sariciftci, *Primary Photoexcitations in Conjugated Polymers: Molecular Exciton versus Semiconductor Band Model* (World Scientific, Singapore, 1997).
[2] J. Burroughes, D. Bradley, A. Brown, R. Marks, K. Mackay, R. Friend, P. Burns, and A. Holmes, Nature (London) **347**, 539 (1990).
[3] C. Yang, K. Lee, and A. Heeger, J. Mol. Struct. **521**, 315 (2000).
[4] D. Comoretto, G. Dellepiane, D. Moses, J. Cornil, D. dos Santos, and J. Brédas, Chem. Phys. Lett. **289**, 1 (1998).
[5] D. Comoretto, G. Dellepiane, F. Marabelli, J. Cornil, D. A. dos Santos, J. L. Brédas, and D. Moses, Phys. Rev. B **62**, 10173 (2000).
[6] C. Soci, D. Comoretto, F. Marabelli, and D. Moses, Phys. Rev. B **75**, 075204 (2007).
[7] M. Galli, F. Marabelli, and D. Comoretto, Appl. Phys. Lett. **86**, 201119 (2005).
[8] C. Soci, D. Comoretto, F. Marabelli, and D. Moses, Proc. SPIE **5517**, 98 (2004).
[9] V. Morandi, C. Soci, M. Galli, F. Marabelli, and D. Comoretto, Optical Probes of Electronic States in Highly Anisotropic Polymeric Semiconductors, in Highlights on Spectroscopies of Semiconductors and Nanostructures, *Conference Proceedings - Italian Physical Society*, edited by G. Guizzetti, M. Patrini, L. C. Andreani, F. Marabelli, Il Nuovo Cimento, Bologna, 2007, Vol. 94, p. 75.
[10] P. K. H. Ho, J. -S. Kim, N. Tessler, and R. H. Friend, J. Chem. Phys. **115**, 2709 (2001).
[11] D. Comoretto, G. Dellepiane, C. Cuniberti, L. Rossi, A. Borghesi, and J. Le Moigne, Phys. Rev. B **53**, 15653 (1996).
[12] D. Comoretto, G. Dellepiane, G. F. Musso, R. Tubino, R. Dorsinville, A. Walser, and R. R. Alfano, Phys. Rev. B **46**, 10041 (1992).
[13] V. Morandi, M. Galli, F. Marabelli, and D. Comoretto, Phys. Rev. B **79**, 045202 (2009).
[14] M. Chandross, S. Mazumdar, M. Liess, P. A. Lane, Z. V. Vardeny, M. Hamaguchi, and K. Yoshino, Phys. Rev. B **55**, 1486 (1997).
[15] M. Chandross and S. Mazumdar, Phys. Rev. B **55**, 1497 (1997).
[16] S. Webster and D. Batchelder, Polymer **37**, 4961 (1996).
[17] M. Chandrasekhar, S. Guha, and W. Graupner, Adv. Mater. **13**, 613 (2001).
[18] S. Guha, W. Graupner, S. Yang, M. Chandrasekhar, H. Chandrasekhar, and G. Leising, Phys. Status Solidi B **211**, 177 (1999).
[19] B. Tian, G. Zerbi, R. Schenk, and K. Müllen, J. Chem. Phys. **95**, 3191 (1991).
[20] B. Tian, G. Zerbi, and K. Müllen, J. Chem. Phys. **95**, 3198 (1991).
[21] J. D. Weibel and D. Yaron, J. Chem. Phys. **116**, 6846 (2002).
[22] E. Palik, *Handbook of Optical Constants of Solids* (Academic, London, 1985).
[23] A. Lang, Nature (London) **213**, 248 (1967).
[24] The calibration measurements at room pressure were performed only on the front diamond of the cell. Notice that a calibration measurement on the whole cell does not provide useful information, being affected by unwanted contributions from the back diamond of the cell and pressure transmitting medium, that are not present in PPV reflectance spectra. Indeed, the PPV film adheres to the front diamond surface. This configurations was necessary to perform reflectance measurements, which require a flat sample surface, perpendicular to the incident beam.
[25] Gaussian functions instead of Lorentzian were found to better reproduce the spectral shape of ϵ_2 due to inhomogeneous broadening effects.
[26] A. Ruini, M. J. Caldas, G. Bussi, and E. Molinari, Phys. Rev. Lett. **88**, 206403 (2002).
[27] J. Gierschner, Y. -S. Huang, B. V. Averbeke, J. Cornil, R. H. Friend, and D. Beljonne, J. Chem. Phys. **130**, 044105 (2009).